0090-9556/08/3605-904–910$20.00
DRUG METABOLISM AND DISPOSITION
Vol. 36, No. 5
18895/3330615
Printed in U.S.A.

DMD 36:904–910, 2008

Two Allelic Variants of Aldo-Keto Reductase *1A1* Exhibit Reduced in Vitro Metabolism of Daunorubicin

Onkar S. Bains, Ryan H. Takahashi, Tom A. Pfeifer, Thomas A. Grigliatti, Ronald E. Reid, and K. Wayne Riggs

Division of Pharmaceutics and Biopharmaceutics, Faculty of Pharmaceutical Sciences, University of British Columbia, Vancouver, British Columbia, Canada (O.S.B., R.H.T., K.W.R.); Life Sciences Institute, Department of Zoology, Faculty of Science, University of British Columbia, Vancouver, British Columbia, Canada (T.A.P., T.A.G.); Division of Biomolecular and Pharmaceutical Chemistry, Faculty of Pharmaceutical Sciences, University of British Columbia, Vancouver, British Columbia, Canada (R.E.R.)

Received September 19, 2007; accepted February 12, 2008

ABSTRACT:

Aldo-keto reductases (AKRs) are a class of NADPH-dependent oxidoreductases that have been linked to metabolism of the anthracyclines doxorubicin (DOX) and daunorubicin (DAUN). Although widely used, cardiotoxicity continues to be a serious side effect that may be linked to metabolites or reactive intermediates generated in their metabolism. In this study we examine the little known effects of nonsynonymous single nucleotide polymorphisms of human *AKR1A1* on the metabolism of these drugs to their alcohol metabolites. Expressed and purified from bacteria using affinity chromatography, the AKR1A1 protein with a single histidine (6x-His) tag exhibited the greatest activity using two test substrates: *p*-nitrobenzaldehyde (5.09 ± 0.16 μmol/min/mg of purified protein) and DL-glyceraldehyde (1.24 ± 0.17 μmol/min/mg). These activities are in agreement with published literature values of nontagged human AKR1A1. The 6x-His-tagged AKR1A1 wild type and allelic variants, E55D and N52S, were subsequently examined for metabolic activity using DAUN and DOX. The tagged variants showed significantly reduced activities (1.10 ± 0.42 and 0.72 ± 0.47 nmol of daunorubicinol (DAUNol) formed/min/mg of purified protein for E55D and N52S, respectively) compared with the wild type (2.34 ± 0.71 nmol/min/mg). The wild type and E55D variant metabolized DOX to doxorubicinol (DOXol); however, the levels fell below the limit of quantitation (25 nM). The N52S variant yielded no detectable DOXol. A kinetic analysis of the DAUN reductase activities revealed that both amino acid substitutions lead to reduced substrate affinity, measured as significant increases in the measured K_m for the reduction reaction by AKR1A1. Hence, it is possible that these allelic variants can act as genetic biomarkers for the clinical development of DAUN-induced cardiotoxicity.

Aldo-keto reductases (AKRs) are a protein superfamily with more than 140 members divided into 15 families (Jin and Penning, 2007). Three of these families, AKR1, AKR6, and AKR7, are found in humans, with AKR1 being the largest (Jin and Penning, 2007; Penning and Drury, 2007). They are widely distributed in human tissues, with high levels of expression being noted in the liver, heart, small intestine, kidney, and brain (O'Connor et al., 1999; Jin and Penning, 2007). AKRs are predominantly monomeric, soluble, NADPH-dependent oxidoreductases involved in the reduction of aldehydes and ketones into primary and secondary alcohols, respectively (Penning and Drury, 2007). Therefore, AKRs are classified as phase I metabolizing enzymes that convert carbonyl groups to alcohols to increase their water solubility for elimination from the body via conjugation reactions.

The AKRs are able to metabolize a broad spectrum of endogenous and exogenous agents. These include monosaccharides, isoflavonoid, steroids, prostaglandins, sugar/lipid aldehydes, polycyclic aromatic hydrocarbons, aflatoxins, and nicotine-derived nitroketones (Penning, 2005). In addition, AKRs have been implicated in the metabolism of the anthracycline antibiotics (Cummings et al., 1991; Jin and Penning, 2007). Since the 1960s, anthracyclines have been used in clinical practice as anticancer drugs in the treatment of leukemias, lymphomas, carcinomas, and sarcomas (Wojtacki et al., 2000; Danesi et al., 2002). Two anthracyclines that are commonly used in cancer treatment are doxorubicin (DOX) and daunorubicin (DAUN). DOX has contributed to improved life expectancy of countless patients affected by cancer, particularly in the treatment of aggressive lymphoma, Hodgkin's disease, childhood solid tumors, soft tissue carcinomas, and breast cancer, whereas DAUN has been administered in patients undergoing treatment for acute myeloid and acute lymphoblastic

This study was supported by a grant from the Canadian Institutes of Health Research (CIHR). R.H.T. was supported by an Rx&D/CIHR scholarship. O.S.B. was supported by a University of British Columbia Graduate Fellowship.

O.S.B. and R.H.T. contributed equally to the experimental studies and writing of this manuscript.

Article, publication date, and citation information can be found at http://dmd.aspetjournals.org.

doi:10.1124/dmd.107.018895.

ABBREVIATIONS: AKR, aldo-keto reductase; DOX, doxorubicin; DAUN, daunorubicin; ns, nonsynonymous; SNP, single nucleotide polymorphism; DOXol, doxorubicinol; DAUNol, daunorubicinol; 6x-His, six histidine; HPLC, high-performance liquid chromatography; FXa, factor Xa; Ni-NTA, nickel-nitrilotriacetic acid; ANOVA, analysis of variance; GST, glutathione *S*-transferase; ROS, reactive oxygen species.

leukemias (Hunault-Berger et al., 2001; Danesi et al., 2002; Fassas and Anagnostopoulos, 2005).

Even though DOX and DAUN therapy has contributed to a longer life in patients with cancer, the clinical use of these anthracyclines has revealed interpatient variability in the development of dose-dependent chronic cardiotoxicity (Wojtacki et al., 2000; Mordente et al., 2001). This form of cardiotoxicity is serious because the effects are irreversible and can often lead to the development of life-threatening complications such as congestive heart failure, cardiomegaly, and decreased left ventricular ejection fractions (Shan et al., 1996; Wojtacki et al., 2000; Simunek et al., 2005). Although the mechanisms by which cardiac tissue damage manifests are not understood, the metabolism of the anthracycline drugs is implicated (Licata et al., 2000; Wojtacki et al., 2000; Menna et al., 2007). Consequently, factors that influence the function of the enzymes responsible for metabolizing these drugs are expected to be determinants in the risk of anthracycline-related cardiotoxicity.

One of the factors underlying the interpatient variation in cardiotoxicity may be linked to ns-SNPs of AKRs responsible for metabolizing DOX and DAUN. Only a few studies have looked at the impact of AKR genetic variants on susceptibility to cancer and other diseases. For example, a higher incidence of lung cancer after exposure to polycyclic aromatic hydrocarbons has been associated with a SNP in *AKR1C3* (Q5H) in the Chinese population (Lan et al., 2004). A SNP in intron 5 of *AKR1A1* has been found to be significantly associated with increased risk of non-Hodgkin's lymphoma (Lan et al., 2007). Genetic variants of *AKR1B1* have been linked to an increased susceptibility to complications in both type 1 and type 2 diabetes (Chung and Chung, 2003; Sivenius et al., 2004; Donaghue et al., 2005). A single nucleotide polymorphism of *AKR1C4* (L311V) led to a significant increase in mammographic density in postmenopausal women, a strong independent risk factor for breast cancer (Lord et al., 2005).

In this study we examined wild-type human AKR1A1 along with the two ns-SNPs, N52S (SNP ID: rs2229540 from National Centre for Biotechnology Information Database) and E55D (SNP ID: rs6690497), in relation to their ability to metabolize DOX and DAUN to their corresponding carbon-13 alcohols, doxorubicinol (DOXol) and daunorubicinol (DAUNol). Using purified bacterially produced recombinant human 6x-His tagged enzymes, we show that the ns-SNPs exhibit significantly reduced activities for the reduction of DAUN compared with the wild type. A kinetic analysis of DAUN reduction demonstrated that the variants maintain similar maximal rates of activity; however, they exhibit reduced substrate affinities. DOX was metabolized by the wild type and variants; however, the levels of DOXol were not quantifiable because they fell below the limit of quantitation. The metabolic differences seen with the variants compared with that of the *AKR1A1* wild type may make N52S and E55D suitable genetic biomarkers in assessing the risk of development of cardiotoxic symptoms in patients with cancer before anthracycline treatment.

Materials and Methods

Chemicals and Enzymes. Agarose, chloramphenicol, daunorubicin, doxorubicin, DL-glyceraldehyde, kanamycin sulfate, lysozyme, methanol, *p*-nitrobenzaldehyde, potassium phosphate (KH_2PO_4) RNase I, sodium phosphate (NaH_2PO_4), *N,N,N′,N′*-tetramethylethylenediamine, and NADPH were supplied by Sigma-Aldrich (St. Louis, MO). HPLC-grade acetonitrile, agar, ammonium persulfate, formic acid, glycine, glycerol, glacial acetic acid, imidazole, and Tris were purchased from Fisher Scientific Co. (Fair Lawn, NJ). NaCl and yeast extract were acquired from EMD Chemicals Inc. (Darmstadt, Germany). Bacto tryptone and isopropyl β-D-1-thiogalactopyranoside (IPTG) were obtained from BD Biosciences (Franklin Lakes, NJ) and Fermentas Inc. (Hanover, MD), respectively. Tween 20 was purchased from EMD Biosciences (La Jolla, CA), and DNase I was provided by Boehringer Manheim GmbH (Manheim, Germany). Klenow fragment and T4 DNA ligase were obtained from Fermentas (Burlington, ON). Restriction enzymes used for this study were purchased from New England Biolabs (Ipswich, MA). Doxorubicinol was obtained from Qventas Inc. (Branford, CT).

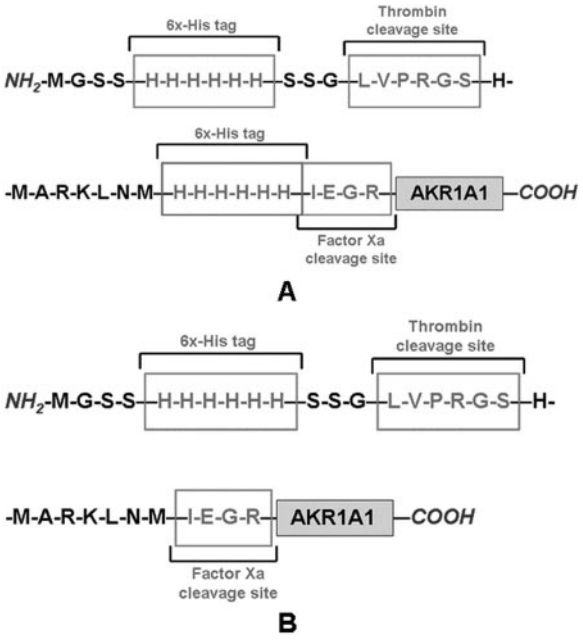

FIG. 1. A translated protein product of the pET28a-*AKR1A1* construct with (A) double 6x-His tags and (B) a single 6x-His tag. The inner 6x-His tag for A was deleted through site-directed mutagenesis.

Molecular Cloning of the Human *AKR1A1* Gene. The insect cell expression vector, *p2Z0p2N*, containing the wild-type *AKR1A1* and the two variant genes were created with a 6x-His tag and factor Xa (FXa) cleavage site on the amino terminus of the AKR gene. The 6x-His tag-FXa-AKR coding regions were excised from the *p2Z0p2N* vector using DraI and NotI and subcloned into the NheI (blunt end with Klenow fragment)-NotI sites of the pET28a (Novagen) prokaryotic expression vector with T4 DNA ligase. These constructs encoded an AKR with two 6x-His tags separated by a 17-amino acid residue linker on the amino terminus (Fig. 1A). The inner 6x-His tag for the pET28a-*AKR1A1* wild type and variant constructs was deleted (Fig. 1B) using the QuikChange Site-Directed Mutagenesis Kit (Stratagene, La Jolla, CA) with the 5′-CCATCCTACCCTCGATCATGTTAAGCTTTCTAG-3′ (forward) and 5′-CTAGAAAGCTTAACATGATCGAGGGTAAGATGG-3′ (reverse) primers. All constructs were verified by dideoxy sequencing at the University of British Columbia Nucleic Acid Protein Service (NAPS) unit.

Expression of Recombinant Human AKR1A1. The pET28a constructs (single and double 6x-His tags) were heat shock-transformed into *Escherichia coli* BL21 (DE3) pLysS and expressed under the control of an IPTG-inducible T7 polymerase. Bacterial cultures (500 ml) were grown at 37°C in LB medium (1% Bacto tryptone, 0.5% yeast extract, and 0.5% NaCl) supplemented with 50 μg/ml kanamycin sulfate and 25 μg/ml chloramphenicol until an OD_{600} of 0.4 was reached. IPTG was added to a final concentration of 1 mM, and cells were allowed to grow for an additional 3 h. Aliquots of cells (1 ml) were collected at 0 (uninduced), 1, 2, and 3 h after IPTG administration for the assessment of AKR1A1 expression levels. The aliquots and cultures remaining after the 3 h of induction were harvested by centrifugation (4000*g* for 20 min ay 4°C), and the resulting bacterial cell pellets were stored at −70°C.

Purification of Recombinant Human AKR1A1. The frozen bacterial pellets were thawed on ice and resuspended at 5 ml/g wet wt. with buffer A (300 mM NaCl and 50 mM NaH_2PO_4, pH 8.0) for the 1-ml aliquots while the suspension from the remaining cultures was further supplemented with 10 mM imidazole. A final concentration of 1 mg/ml lysozyme was added to all of the cell suspensions, followed by incubation on ice for 30 min. Cells were disrupted using six 10-s bursts (with a 10-s cooling period between each burst) from a sonic dismembranator with a microtip set at 200 to 300 W. This was

followed by incubation with DNase I and RNase I (5 and 10 μg/ml, respectively) for 15 min on ice and then centrifugation (10,000*g* for 20 min at 4°C). The cell lysate supernatants of the aliquots collected from 0 to 3 h were saved for Western blot analysis, whereas the lysate from the remaining culture was subjected to Ni-NTA affinity chromatography, with the recombinant protein being isolated according to the manufacturer's instructions (QIAGEN, Mississauga, ON, Canada). Briefly, the supernatant was incubated with Ni-NTA agarose beads for 1.5 h at 4°C, and the mixture was transferred into a column. The 6x-His-tagged AKR1A1 protein bound to the agarose beads was washed with multiple fractions (2.5 bed volumes/fraction) of buffer A containing 20 mM imidazole to remove nonspecific endogenous bacterial proteins bound to the beads, which was monitored by measuring the total protein concentration of each fraction using the Bio-Rad Protein Assay (Hercules, CA). AKRs were further eluted with multiple fractions of buffer A with 30, 50, 100, and 250 mM imidazole. At each of these imidazole concentrations, fractions (0.75 bed volume) were collected until the total protein dropped to baseline levels. Glycerol was added to the elution fractions to a final concentration of 20% and the samples stored at −20°C.

Total Protein Staining. Purity of the AKR1A1 elution fractions was assessed visually after electrophoresis using an 18% SDS-polyacrylamide gel and staining for total protein. The gels were fixed in 50% methanol and 7% glacial acetic acid for two periods of 30 min each and then stained with SYPRO Ruby (Invitrogen Canada, Inc., Burlington, ON, Ontario) overnight. After staining, the gels were washed in 10% methanol and 7% glacial acetic acid for 30 min, and the protein detected using a Storm 860 Molecular Imager (GMI Inc., Ramsey, MN).

Western Blotting. Western blot analyses of the cell lysates from the aliquots and the purified fractions were performed according to the protocol described by Odyssey (LI-COR Biosciences, Lincoln, NE). After an 18% SDS-polyacrylamide gel electrophoresis, proteins were transferred in Towbin's buffer (25 mM Tris, 192 mM glycine, and 20% v/v methanol) overnight at 20 to 30 V to a Hybond-C Extra nitrocellulose membrane (GE Healthcare, Piscataway, NJ). The membranes were blocked in Odyssey blocking buffer (BB), and the enzyme was detected using a monoclonal mouse anti-human AKR1A1 (Abnova Corporation, Taipei City, Taiwan) antibody (diluted 1:5000) as the primary antibody and IRDye 800CW goat anti-mouse IgG as the secondary antibody (diluted 1:5000) (LI-COR). Both primary and secondary antibodies were in BB containing 0.1% Tween 20. The bound secondary antibodies were detected using the Odyssey Infrared Imaging system (LI-COR Biosciences).

AKR1A1 Enzymatic Activity Assays. The activity of the purified single and double 6x-His-tagged AKR1A1 was measured at 25°C using a Fluoroskan Ascent FL (Thermo Fisher Scientific, Waltham, MA) by following the initial rate of NADPH oxidation at excitation and emission wavelengths of 355 and 460 nm, respectively. The assays were conducted as described previously for the characterization of AKR proteins (Palackal et al., 2001). In short, purified protein was incubated with 180 μM NADPH and 1 mM test substrate, either *p*-nitrobenzaldehyde or DL-glyceraldehyde, in a reaction mixture of 150 μl of 100 mM potassium phosphate, pH 7.0, at 25°C. Protein amounts and incubation times were selected for each enzyme and substrate concentration to ensure that measured rates were in the linear range of the enzyme kinetic curve. In these assays, the concentration of organic solvent, which was required to dissolve the substrate, was kept below 4% (v/v) in the final reaction mixture. Readings were collected at 1-min intervals for 3 h with shaking between each reading. Maximal rates were calculated from the Ascent program (version 2.6) using a 5-min interval with the steepest slope. Enzymatic activity (micromoles of NADPH consumed per minute per milligram of purified protein) was calculated from these rates using a standard curve constructed from the fluorescence measurements of solutions of known NADPH concentrations.

Activity measurements for DAUN reduction were performed by incubating either DOX or DAUN with purified AKR1A1 protein in a total volume of 150 μl containing 25 mM potassium phosphate, pH 7.4, and 1 mM NADPH at 37°C. Protein concentrations were based on the Bradford protein assay using bovine serum albumin as a standard. The reaction was stopped by adding 300 μl of ice-cold acetonitrile, which contained idarubicin as an internal standard, followed by vortex mixing and centrifuging at 10,000*g* for 10 min at 4°C to remove protein. The supernatant was removed for HPLC analysis. HPLC separation was performed using a Waters Alliance 2695 system (Waters Corporation, Milford, MA) with an analytical column (Waters Symmetry C18, 75 × 4.6 mm i.d., 3 μm) and guard column (Phenomenex SecurityGuard C18, 40 × 4.6 mm i.d.; Phenomenex, Torrance, CA). HPLC conditions were as follows: mobile phase A, 0.1% formic acid and B, acetonitrile; gradient elution, 0 to 1 min, 15% B; 1 to 8 min, 15% B to 35% B; 8 to 10 min, 35% B; 10 to 10.1 min, 35% B to 15% B; column re-equilibration for 2 min at a constant flow rate of 1 ml/min. The column was heated to 30°C and the autosampler temperature was set to 10°C with 5 μl of sample injected onto the column. Fluorescence detection of DOX and DAUN and their carbon-13 hydroxy metabolites was performed with excitation and emission wavelengths of 460 and 550 nm, respectively (Waters 2475 Multi λ Detector).

Quantitation of DOXol and DAUNol was performed on the basis of a weighted ($1/x^2$) linear regression determined from solutions of known concentrations of an authentic chemical standard for DOXol. Because a chemical standard for DAUNol could not be obtained, its concentrations were calculated as DOXol equivalents using a response ratio of 1.0. All HPLC data processes, including chromatogram integration, calibration, and quantitative calculations, were performed with Waters Empower software (version 2.0).

The kinetic constants of maximal rate of reaction, V_{max}, and K_m were determined by fitting rate measurement data using nonlinear least-squares fitting of a Michaelis-Menten hyperbola (GraphPad Prism version 4.0; GraphPad Software Inc., San Diego, CA). k_{cat} values were calculated from V_{max} values using the apparent molecular weight for the 6x-His-tagged AKR protein of 41,000.

Statistical Analysis. Statistical analyses were performed using GraphPad Instat (version 3.6; GraphPad Software Inc.). Results are expressed as means ± S.D. Enzyme activities were compared using a one-way ANOVA followed by Tukey-Kramer multiple comparisons tests. Differences were considered significant at $p < 0.05$.

Results

Expression and Purification. Successful expression of the single and double 6x-His-tagged human AKR1A1 was obtained and visualized by performing a Western blot on the noninduced and IPTG-induced (1, 2, and 3 h) cell lysates from the aliquots that were collected during the growth of the bacterial cultures. To purify the wild type and ns-SNPs to homogeneity, the lysates from the 3-h induced cultures were subjected to affinity chromatography yielding fractions containing the 6x-His tagged AKR1A1 without the presence of detectable contaminating proteins (Fig. 2). The majority of pure enzyme was recovered in the elution fractions with 50 and 250 mM imidazole for the single and double 6x-His-tagged enzymes, respectively. The bands for each of the purified samples have a mobility corresponding to the relative molecular mass of the 6x-His tagged AKR1A1, which is ~41,000 to42,000. The identities of these fractions were verified by Western blot analysis (Fig. 2).

Characterization of AKR1A1 Using Enzymatic Activities with Test Substrates. The single 6x-His-tagged AKR1A1 wild type had greater metabolic activities for *p*-nitrobenzaldehyde and DL-glyceraldehyde compared with the enzyme tagged with double 6x-His or the glutathione *S*-transferase (GST)-tagged wild-type construct (Abnova Corporation) (Fig. 3). The reaction rates for the single 6x-His-tagged wild-type AKR1A1 were 5.09 ± 0.16 and 1.24 ± 0.17 μmol NADPH consumed/min/mg of purified protein for *p*-nitrobenzaldehyde and DL-glyceraldehyde, respectively. These values were in accordance with the reaction rates of bacterially expressed recombinant human untagged AKR1A1 reported in the literature using identical or comparable assays: 6.0 μmol/min/mg for *p*-nitrobenzaldehyde and 1.26 μmol/min/mg for DL-glyceraldehyde (O'Connor et al., 1999; Palackal et al., 2001). This finding suggests that the amino acid linker and 6x-His tag engineered on the N terminus of the AKR gene has no significant effect on the enzyme activity. Therefore, the recovery tag does not need to be cleaved off with FXa for subsequent activity assays involving the anthracyclines. Enzyme activity measurements of

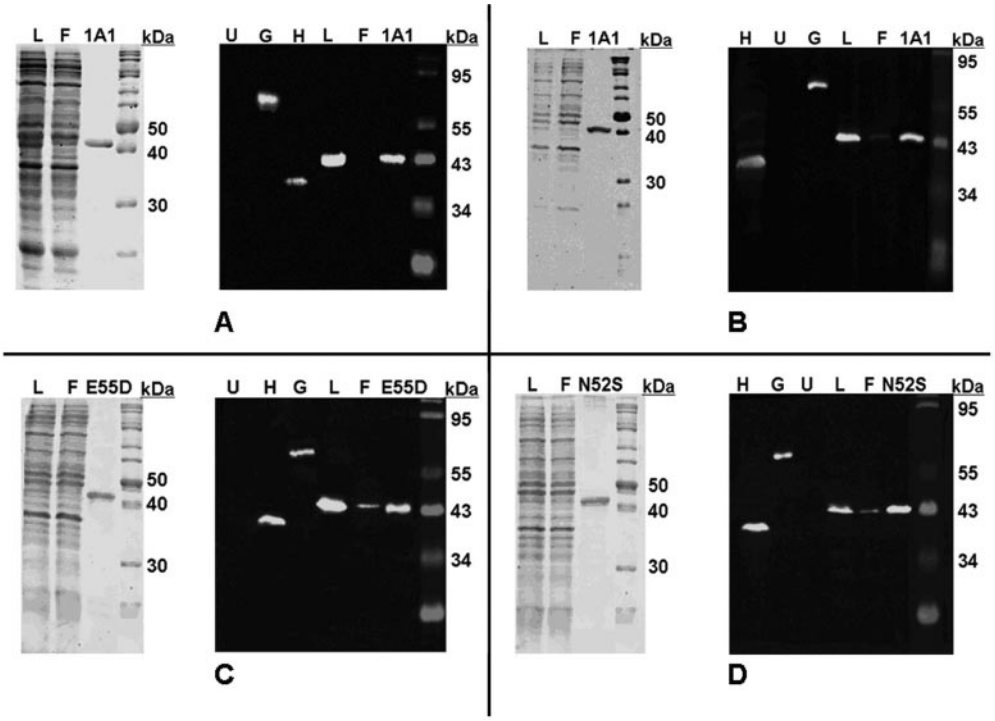

FIG. 2. Purification of human recombinant (A) double 6x-His-tagged AKR1A1 wild-type, (B) single 6x-His-tagged AKR1A1 wild-type, (C) E55D variant, and (D) N52S variant enzymes. Left, gels stained with SYPRO Ruby after SDS-polyacrylamide gel electrophoresis showing purified protein samples, 1A1 wild type, and variants (700 ng), free of contaminating proteins from bacterial lysates (L) (20 μg of total protein). Removal of contaminating proteins is observed in fractions from QIAGEN purification procedures [Ni-NTA column flow through (F), 15 μg of total protein]. Right, Western blot detection of purified protein samples, 1A1 wild type, and variants (700 ng) confirms expression of the desired AKR protein with mobility at expected molecular weight (~41,000–42,000). Positive controls for antibody immunoreactivity are human liver cytosol (H; 20 μg of total protein) and GST-tagged purified human recombinant AKR enzymes (G; 700 ng). No antibody immunoreactivity is observed for untransformed bacterial lysate (U; 20 μg of total protein).

the single 6x-His-tagged E55D allelic variant demonstrated significantly reduced metabolic activity with *p*-nitrobenzaldehyde, whereas both ns-SNPs had significantly reduced activity with DL-glyceraldehyde (Fig. 4). The enzymatic rates for reductions of *p*-nitrobenzaldehyde and DL-glyceraldehyde for the E55D variant were 1.04 ± 0.26 and 0.52 ± 0.17 μmol/min/mg, respectively, whereas the N52S variant had rates of 5.00 ± 0.41 and 0.85 ± 0.17 μmol/min/mg.

AKR1A1 Activity with Anthracyclines. To evaluate the impact of the single amino acid substitutions on the reduction of the anthracycline drugs by AKR1A1, we measured the formation of the alcohol metabolites in vitro. The in vitro conditions were selected to reflect physiological conditions (i.e., pH 7.4 at 37°C), and both DAUN and DOX were studied. Full chromatographic resolution of DAUNol and DOXol from DAUN, DOX, and idarubicin (internal standard) was achieved for all chemical standards and in vitro samples. DOXol, DOX, DAUNol, DAUN, and idarubicin were observed to elute at 4.5, 5.5, 6.0, 6.8, and 7.3 min, respectively. Incubation of the single 6x-His-tagged AKR1A1 protein with DOX generated a single new chromatographic peak that was identified as DOXol. Similarly, incubation with DAUN generated a single new chromatographic peak that was identified as DAUNol. The identification of the metabolite peaks was confirmed by incubation of DOX and DAUN with human liver cytosol and the generation of compounds that had identical chromatographic behaviors, as well as correspondence in retention time of the metabolite peak from DOX incubations with that for the chemical standard of DOXol. No detectable amounts of DAUNol or DOXol were found in incubations conducted in the absence of protein.

Specific activity measurements were performed to compare the anthracycline reductase function of the single 6x-His-tagged AKR1A1 wild-type and ns-SNP variant proteins. Specific activities for the wild-type, N52S, and E55D proteins were determined as 2.34 ± 0.71, 0.72 ± 0.47, and 1.10 ± 0.42 nmol/min/mg of protein, respectively, using DAUN as the substrate at an initial concentration of 1 μM (Fig. 5). For DOXol, metabolite was only observed to form after 120 or 240 min by one 6x-His tagged AKR1A1 wild-type and E55D samples, but the amount of metabolite produced over that time

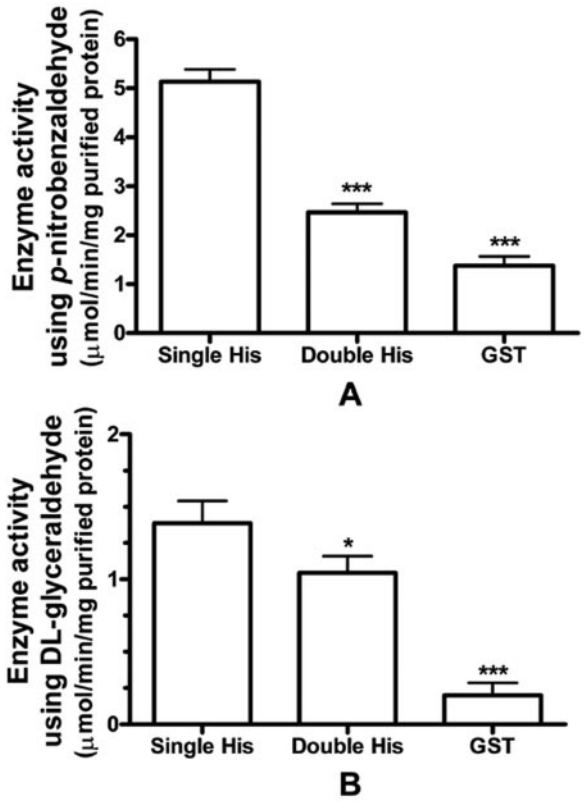

FIG. 3. In vitro enzymatic activities for the purified single and double 6x-His-tagged AKR1A1 wild types along with the GST-tagged AKR1A1 wild type in the presence of 1 mM (A) *p*-nitrobenzaldhyde and (B) DL-glyceraldehyde test substrates as measured by following the initial rate of NADPH oxidation. A single batch of each enzyme was purified with assays being performed in triplicate for each batch. Enzymatic activities are reported as mean ± S.D. ($n = 3$) with the background levels subtracted. The background levels represented the reaction buffer, enzyme and NADPH cofactor only, without the addition of the test substrate. *, $p < 0.05$; ***, $p < 0.001$; significantly different from the single 6x-His-tagged treatment group by one-way ANOVA followed by Tukey-Kramer multiple comparisons tests.

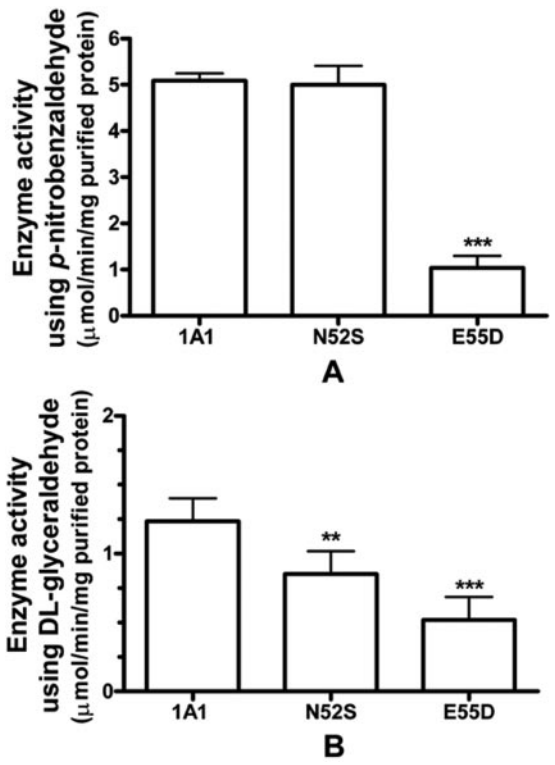

FIG. 4. In vitro enzymatic activities for the purified single 6x-His-tagged AKR1A1 wild-type and ns-SNP variants with 1 mM (A) *p*-nitrobenzaldehyde and (B) DL-glyceraldehyde test substrates as measured by following the initial rate of NADPH oxidation. Three independent batches of each enzyme were purified. Assays were performed in quadruplicate with each batch. Enzymatic activities are reported as mean ± S.D. ($n = 12$) with the background levels subtracted. The background levels represented the reaction buffer, enzyme, and NADPH cofactor only, without the addition of the test substrate. **, $p < 0.01$; ***, $p < 0.001$; significantly different from the wild-type treatment group by one-way ANOVA followed by Tukey-Kramer multiple comparisons tests.

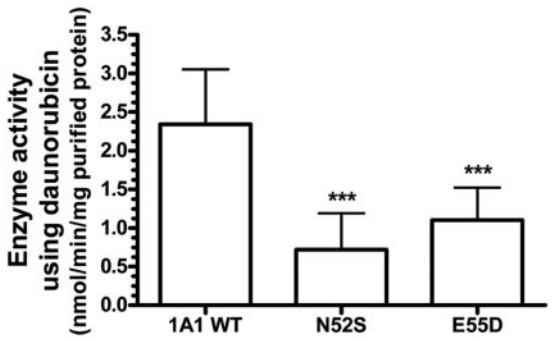

FIG. 5. Generation of DAUNol in vitro of purified single 6x-His-tagged AKR1A1 wild-type (WT) and ns-SNP variants. Measurement of DAUNol was performed using HPLC fluorescence detection. Three independent batches of each enzyme were purified. Assays were performed in triplicate with each batch. Enzymatic activities are reported as mean ± S.D. ($n = 9$). ***, $p < 0.001$; significantly different from wild-type treatment group by one-way ANOVA followed by Tukey-Kramer multiple comparisons tests.

was less than the lower limit of quantification (25 nM) for the HPLC assay. No DOXol metabolite was observed using the tagged N52S allelic variant.

To further understand the functional consequences of the single amino acid substitutions on anthracycline metabolism, we performed kinetic studies using DAUN as a prototype for anthracycline drugs, at concentrations from 12.5 to 1250 μM. It was noted during the experiments that some extrapolation of the enzyme kinetic curves was necessary to estimate V_{max} and K_m parameters; however, complete saturation with higher substrate concentrations was not feasible experimentally because of analytical and limited substrate constraints. We observed similar maximal rates of velocity, but the K_m values for the N52S and E55D were both increased by approximately 2-fold (Table 1). The reduced substrate affinities of these enzymes from the wild-type isoform are in good agreement with the differences we observed in specific activity for DAUN in vitro at a 1 μM concentration.

TABLE 1

Kinetic constants for DAUN reduction by recombinant AKR1A1 wild-type and variant allele proteins

Values correspond to mean ± S.D. obtained from three experiments performed with three independent protein preparations ($n = 9$) for each isoform.

Kinetic Parameter	AKR1A1		
	Wild type	N52S	E55D
K_m (mM)	1.2 ± 0.3	2.3 ± 0.9*	2.3 ± 1.1*
V_{max} (μmol/min · mg protein)	4.4 ± 0.5	4.3 ± 2.0	3.1 ± 1.0
k_{cat} (s^{-1})[a]	3.0	2.1	3.0
k_{cat}/K_m (s^{-1} M^{-1})	2.5×10^3	9.3×10^2	1.3×10^3

* Significantly different from wild type ($P < 0.05$).
[a] k_{cat} calculated from M_r 41,000.

Discussion

AKRs play a fundamental role in the metabolism of a wide array of carbonyl-containing compounds that are either endogenous or exogenous in nature. However, few studies have examined the effect of genetic polymorphisms of specific AKRs on physiological and biomolecular processes that can lead to increased or decreased susceptibility to human-related diseases. To our knowledge, this article describes the first experimental finding of the altered metabolism of DOX and DAUN by the single 6x-His-tagged human AKR1A1 (wild type and ns-SNPs). These anthracyclines have contributed to improved life expectancy in countless patients with cancer through different mechanisms such as topoisomerase II inhibition, DNA intercalation, induction of cell apoptosis, and RNA synthesis inhibition (Minotti et al., 2004; Rabbani et al., 2005). In this study, in vitro metabolic assays using purified AKR1A1, which was expressed and induced in *E. coli*, were conducted with DOX and DAUN. Incubations with test substrates, *p*-nitrobenzaldehyde and DL-glyceraldehyde, were performed to ensure that purified enzyme was fully functional. The water-soluble carbon-13 alcohol metabolites, DOXol and DAUNol, were selected for analysis because previous studies have acknowledged them to be the major metabolites in patients (Lipp and Bokemeyer, 1999; Plebuch et al., 2007). It was shown that DOX is a poor substrate for the single 6x-His tagged AKR1A1, unlike DAUN, which is readily metabolized to its respective carbon-13 metabolite. This is an interesting finding because the chemical structures of DOX and DAUN are highly similar (Fig. 6). This higher metabolic activity for DAUN compared with DOX is in agreement with what has been observed in vitro for formation of the alcohol metabolites by cytosolic fractions prepared from human cardiac tissue (Mordente et al., 2001). It would appear that AKR1A1 has high specificity for DAUN over DOX even though these anthracyclines are structurally similar.

The amino acid linker modification of AKR1A1 was essential in exposing the 6x-His tag to the Ni-NTA resin for successful purification using Ni-NTA affinity chromatography. By using the single and double 6x-His-tagged wild-type and variant enzymes, our intent was to remove the tag(s) and amino acid linker using FXa, which cleaves after the arginine residue in the IEGR recognition sequence, to produce the native AKR1A1. This attempt was unsuccessful with substantial cleavage occurring at a secondary site (data not shown). It is

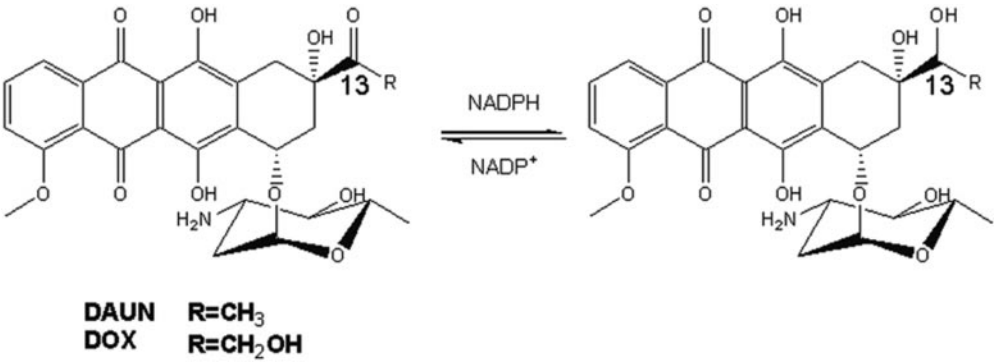

FIG. 6. Chemical structures of DOX and DAUN and their conversion to their corresponding carbon-13 alcohol metabolites, DOXol and DAUNol.

likely that the FXa cleavage site was hidden within the protein structure, thereby making it inaccessible for recognition by the FXa enzyme. The following attempts to remove the 6x-His tag by FXa cleavage optimization were undertaken: 1) altering concentrations of the reaction buffer components, Tris-HCl, $CaCl_2$, and NaCl; 2) using different ranges of pH (6–9) and temperature (4–37°C) to increase FXa specificity; 3) increasing FXa enzyme concentration; and 4) incubating the 6x-His tagged protein with thrombin to cleave the tag and a portion of the linker at the thrombin recognition site, which may alter the folding of AKR1A1 and expose the primary cleavage site for FXa. Secondary site cleavage was also seen when FXa incubations were conducted while the enzyme was bound to the Ni-NTA resin. However, as stated earlier, the activities of the single 6x-His tagged wild-type enzyme were in accordance with activity values of non-tagged human AKR1A1 as reported in literature using comparable assays. This was not the case for the double 6x-His-tagged enzymes, which were demonstrated to have lower activity when the test substrates were used. We deemed it unnecessary to cleave the tag and linker from single 6x-His-tagged AKR1A1 as they did not appear to alter enzyme activity.

The single 6x-His-tagged ns-SNP variants were demonstrated to have significantly reduced catalytic activity compared with that of the single 6x-His-tagged wild type. Reduction of the carbonyl group by AKR enzymes is thought to involve the cooperation of four amino acids (tyrosine, lysine, aspartic acid, and histidine), which form a catalytic tetrad. These four amino acids and their positions are conserved in the vast majority of the individual reductases within this superfamily (Jez et al., 1997; Penning 2001). In the case of AKR1A1, these amino acids would be found in the following positions: aspartic acid-45, tyrosine-50, lysine-85, and histidine-113. The phenolic hydroxyl group of tyrosine is considered to be the most likely candidate to function as the general acid/base catalyst of the reaction with AKR1A1 substrates, whereas the other amino acid residues appear to have auxiliary roles in catalysis (Schlegel et al., 1998; Di Luccio et al., 2006; Jin and Penning, 2007). Because the single amino acid changes seen with the two ns-SNPs, N52S and E55D, occur close to the catalytic tyrosine-50 residue, it is possible that these changes hinder the catalytic role of tyrosine-50 in the metabolism of the anthracyclines and the test substrates. Although the chemical properties are mostly retained in these amino acids substitutions (N52S: both residues are hydrophilic; E55D: both residues are negatively charged and hydrophilic), the size and shape differences in the amino acid side chains may affect the structure of the active site of the enzyme, thereby altering the efficiency of the metabolic process.

It is quite possible that the observed metabolic activity differences between the single 6x-His tagged AKR1A1 wild-type and allelic variants are reflected in the large interindividual variability seen with DOX- or DAUN-induced cardiotoxicity. We observed that the N52S and E55D substitutions result in a reduction of approximately 50% in catalytic efficiency (k_{cat}/K_m) of the AKR1A1 enzyme because of changes in substrate affinity. This finding suggests that the efficiency of anthracycline alcohol metabolite formation via these enzymes per unit time will be dramatically reduced in patients that carry this ns-SNP. There are several proposed mechanisms of anthracycline-induced cardiotoxicity, which include cellular toxicity from metabolites, selective inhibition of gene expression for proteins associated with contraction of the myocardium, and inhibition of topoisomerase II activity (Boucek et al., 1987; Ito et al., 1990; Cummings et al., 1991; Minotti et al., 1995; Mordente et al., 2001; Adamcova et al., 2003). Although the cause of cardiotoxicity is probably multifactorial, most studies support the view that an increase in reactive oxygen species (ROS) plays a key role in the pathogenesis of anthracycline-induced cardiomyocyte damage (Doroshow 1983; Rajagopalan et al., 1988; Yen et al., 1996; Arai et al., 2000; Singal et al., 2000; Kim et al., 2005; Wold et al., 2005). ROS are a major concern since they are capable of deleterious effects such as oxidation of cell membrane lipids, defects of the mitochondrial respiratory chain, DNA disintegration, and dysfunction of enzymes containing sulfhydryl groups, all of which contribute to chronic cardiotoxicity (Wojtacki et al., 2000). ROS generation in the presence of DOX and DAUN is speculated to occur through metabolic processes involving oxidoreductases such as the AKRs (Tokarska-Schlattner et al., 2006). Therefore, it is conceivable that certain AKR alleles can contribute to a substantially higher, or lower, risk of producing ROS. Currently, we are looking at ROS formation via AKR1A1 (wild type and ns-SNPs) to see whether there is correlation with DOX and DAUN metabolism.

In conclusion, this study illustrates that a one 6x-His-tagged AKR1A1 enzyme with activity similar to that of the untagged enzyme is an efficient metabolizer of DAUN and has little to no activity on DOX. We have also demonstrated here that the two naturally occurring allelic variations in *AKR1A1* lead to reduced reductase activity toward DAUN as a substrate. Hence, the N52S and/or E55D SNPs in *AKR1A1* may prove to be useful genetic biomarkers for assessing the risk of development of cardiotoxicity in patients with cancer before treatment. Individuals treated with DAUN who carry one or both of these alleles would be expected to have a reduced ability to eliminate DAUN via this pathway, consequently, leading to its metabolism by a less favorable pathway and thus the generation of other harmful metabolites or reactive intermediates. Studies to support these hypotheses are currently underway in our laboratory.

Acknowledgments. The authors extend their gratitude to Dr. R. C. Mottus, Dr. J. W. Hodgson, J. G. Doheny, O. Toub, P. Kalas, and M. A. Earp for their advice and technical assistance.

References

Adamcova M, Pelouch V, Gersl V, Kaplanova J, Mazurova Y, Simunek T, Klimtova I, and Hrdina R (2003) Protein profiling in daunorubicin-induced cardiomyopathy. *Gen Physiol Biophys* **22:**411–419.

Arai M, Yoguchi A, Takizawa T, Yokoyama T, Kanda T, Kurabayashi M, and Nagai R (2000) Mechanism of doxorubicin-induced inhibition of sarcoplasmic reticulum Ca^{2+}-ATPase gene transcription. *Circ Res* **86:**8–14.

Boucek RJ Jr, Olson RD, Brenner DE, Ogunbunmi EM, Inui M, and Fleischer S (1987) The major metabolite of doxorubicin is a potent inhibitor of membrane-associated ion pumps: a correlative study of cardiac muscle with isolated membrane fractions. *J Biol Chem* **262:**15851–15856.

Chung SS and Chung SK (2003) Genetic analysis of aldose reductase in diabetic complications. *Curr Med Chem* **10:**1375–1387.

Cummings J, Anderson L, Willmott N, and Smyth JF (1991) The molecular pharmacology of doxorubicin *in vivo. Eur J Cancer* **27:**532–535.

Danesi R, Fogli S, Gennari A, Conte P, and Del Tacca M (2002) Pharmacokinetic pharmacodynamic relationships of the anthracycline anticancer drugs. *Clin Pharmacokinet* **41:**431–444.

Di Luccio E, Elling RA, and Wilson DK (2006) Identification of a novel NADH-specific aldo-keto reductase using sequence and structural homologies. *Biochem J* **400:**105–114.

Donaghue KC, Margan SH, Chan AK, Holloway B, Silink M, Rangel T, and Bennetts B (2005) The association of aldose reductase gene (*AKR1B1*) polymorphisms diabetic neuropathy in adolescents. *Diabet Med* **22:**1315–1320.

Doroshow JH (1983) Effect of anthracycline antibiotics on oxygen radical formation in rat heart. *Cancer Res* **43:**460–472.

Fassas A and Anagnostopoulos A (2005) The use of liposomal daunorubicin (DaunoXome) in acute myeloid leukemia. *Leuk Lymphoma* **46:**795–802.

Hunault-Berger M, Milpied N, Bernard M, Jouet JP, Delain M, Desablens B, Sadoun A, Guilhot F, Casassus P, and Ifrah N (2001) Daunorubicin continuous infusion induces more toxicity than bolus infusion in acute lymphoblastic leukemia induction regimen: a randomized study. *Leukemia* **15:**898–902.

Ito H, Miller SC, Billingham ME, Akimoto H, Torti SV, Wade R, Gahlmann R, Lyons G, Kedes L, and Torti FM (1990) Doxorubicin selectively inhibits muscle gene expression in cardiac muscle cells *in vivo* and *in vitro. Proc Natl Acad Sci U S A* **87:**4275–4279.

Jez JM, Bennett MJ, Schlegel BP, Lewis M, and Penning TM (1997) Comparative anatomy of the aldo-keto reductase superfamily. *Biochem J* **326:**625–636.

Jin Y and Penning TM (2007) Aldo-keto reductases and bioactivation/detoxification. *Ann Rev Pharmacol Toxicol* **47:**10.1–10.30.

Kim DS, Kim HR, Woo EF, Hong ST, Chae HJ, and Chae SW (2005) Inhibitory effects of rosmarinic acid on Adriamycin-induced apoptosis in H9c2 cardiac muscle cells by inhibiting reactive oxygen species and the activations of c-Jun N-terminal kinase and extracellular signal-regulated kinase. *Biochem Pharmacol* **70:**1066–1078.

Lan Q, Mumford JL, Shen M, Demarini DM, Bonner MR, He X, Yeager M, Welch R, Chanock S, Tian L, et al. (2004) Oxidative damage-related genes AKR1C3 and OGG1 modulate risks for lung cancer due to exposure to PAH-rich coal combustion emissions. *Carcinogenesis* **25(11):**2177–2181.

Lan Q, Zheng T, Shen M, Zhang Y, Wang SS, Zahm SH, Holford TR, Leaderer B, Boyle P, and Chancock S (2007) Genetic polymorphisms in the oxidative stress pathway and susceptibility to non-Hodgkin lymphoma. *Hum Genet* **121:**161–168.

Licata S, Saponiero A, Mordente A, and Minotti G (2000) Doxorubicin metabolism and toxicity in human myocardium: role of cytoplasmic deglycosidation and carbonyl reduction. *Chem Res Toxicol* **13:**414–420.

Lipp HP and Bokemeyer C (1999) Anthracyclines and other intercalating agents, in *Anticancer Drug Toxicity: Prevention, Management and Clinical Pharmacokinetics* (Lipp HP ed) pp 81–113, Marcel Dekker, New York.

Lord SJ, Mack WJ, Van Den Berg D, Pike MC, Ingles SA, Haiman CA, Wang W, Parisky YR, Hodis HN, and Ursin G (2005) Polymorphisms in genes involved in estrogen and progesterone metabolism and mammographic density changes in women randomized to postmenopausal hormone therapy: results from a pilot study. *Breast Cancer Res* **7:**R336–R344.

Menna P, Recalcati S, Cairo G, and Minotti G (2007) An introduction to the metabolic determinants of anthracycline cardiotoxicity. *Cardiovasc Toxicol* **7:**80–85.

Minotti G, Cavaliere AF, Mordente A, Rossi M, Schiavello R, Zamparelli R, and Possati G (1995) Secondary alcohol metabolites mediate iron delocalization in cytosolic fractions of myocardial biopsies exposed to anticancer anthracyclines: novel linkage between anthracycline metabolism and iron-induced cardiotoxicity. *J Clin Invest* **95:**1595–1605.

Minotti G, Menna P, Salvatorelli E, Cairo G, and Gianni L (2004) Anthracyclines: molecular advances and pharmacologic developments in antitumor activity and cardiotoxicity. *Pharmacol Rev* **56:**185–229.

Mordente A, Meucci E, Martorana GE, Giardina B, and Minott G (2001) Human heart cytosolic reductases and anthracycline cardiotoxicity. *IUBMB Life* **52:**83–88.

O'Connor T, Ireland LS, Harrison DJ, and Hayes JD (1999) Major differences exist in the function and tissue-specific expression of human aflatoxin B1 aldehyde reductase and the principal human aldo-keto reductase AKR1 family members. *Biochem J* **343:**487–504.

Palackal NT, Burczynski ME, Harvey RG, and Penning TM (2001) The ubiquitous aldehyde reductase (AKR1A1) oxidizes proximate carcinogen *trans*-dihydrodiols to *o*-quinones: Potential role in polycyclic aromatic hydrocarbon activation. *Biochemistry* **40:**10901–10910.

Penning TM (2005) Introduction and overview of the aldo-keto reductase superfamily, in *Aldo-Keto Reductases and Toxicant Metabolism* (Penning TM and Petrash JM eds) pp 3–20, American Chemical Society, Washington DC.

Penning TM and Drury JE (2007) Human aldo-keto reductases: function, gene regulation, and single nucleotide polymorphisms. *Arch Biochem Biophys* **464:**241–250.

Plebuch M, Soldan M, Hungerer C, Koch L, and Maser E (2007) Increased resistance of tumor cells to daunorubicin after transfection of cDNAs coding for anthracycline inactivating enzymes. *Cancer Lett* **255:**49–56.

Rabbani A, Finn RM, and Ausio J (2005) The anthracycline antibiotics: antitumor drugs that alter chromatin structure. *Bioassays* **27:**50–56.

Rajagopalan S, Politi PM, Sinha BK, and Myers CE (1988) Adriamycin-induced free radical formation in the perfused rat heart: implications for cardiotoxicity. *Cancer Res* **48:**4766–4769.

Schlegel BP, Jez JM, and Penning TM (1998) Mutagenesis of 3α-hydroxysteroid dehydrogenase reveals a "push-pull" mechanism for proton transfer in aldo-keto reductases. *Biochemistry* **37:**3538–3548.

Shan K, Lincoff AM, and Young JB (1996) Anthracycline-induced cardiotoxicity. *Ann Intern Med* **125:**47–58.

Simunek T, Klimtova L, Kaplanova J, Sterba M, Mazurova Y, Adamcova M, Hrdina R, Gersl V, and Ponka P (2005) Study of daunorubicin cardiotoxicity prevention with pyridoxal isonicotinoyl hydrazone in rabbits. *Pharmacol Res* **51:**223–231.

Singal PK, Li T, Kumar D, Danelisen I, and Iliskovic N (2000) Adriamycin-induced heart failure: mechanism and modulation. *Mol Cell Biochem* **207:**77–85.

Sivenius K, Niskanen L, Voutilainen-Kaunisto R, Laakso M, and Uusitupa M (2004) Aldose reductase gene polymorphisms and susceptibility to microvascular complications in type 2 diabetes. *Diabet Med* **21:**1325–1333.

Tokarska-Schlattner M, Zaugg M, Zuppinger C, Wallimann T and Schlattner U (2006) New insights into doxorubicin-induced cardiotoxicity: the critical role of cellular energetics. *J Mol Cell Cardiol* **41:**389–405.

Wojtacki J, Lewicka-Nowak E, and Lesniewski-Kmak K (2000) Anthracycline-induced cardiotoxicity: clinical course, risk factors, pathogenesis, detection and prevention review of the literature. *Med Sci Monit* **6:**411–420.

Wold LE, Aberle NS, and Ren J (2005) Doxorubicin induces cardiomyocyte dysfunction via a p38 MAP kinase-dependent oxidative stress mechanism. *Cancer Detect Prev* **29:**294–299.

Yen HC, Oberley TD, Vichitbandha S, Ho YS, and St Clair DK (1996) The protective role of manganese superoxide dismutase against Adriamycin-induced acute cardiac toxicity in transgenic mice. *J Clin Invest* **98:**1253–1260.

Address correspondence to: Dr. K. Wayne Riggs, Division of Pharmaceutics and Biopharmaceutics, Faculty of Pharmaceutical Sciences, 2146 East Mall, University of British Columbia, Vancouver, BC, Canada V6T 1Z3. E-mail: riggskw@interchange.ubc.ca